Gasdynamic Effects of Shock-Flame Interactions in an Explosive Gas

A. J. LADERMAN,* P. A. URTIEW,† AND A. K. OPPENHEIM‡
University of California, Berkeley, Calif.

Previous studies of the shock-flame interaction processes are critically reviewed. Experimental observations reported in the literature are analyzed by means of the vector polar method, which provides information on the stationary states produced by the interactions rather than on the processes that occur in the course of their progress. Results of our experimental study performed with the use of hydrogen-oxygen mixtures at low initial pressures are then presented and interpreted by the use of the same method of analysis. The study leads to the following conclusions: 1) a satisfactory explanation of the interaction effects can be obtained on the basis of gasdynamic analysis, provided that proper allowance is made for the finite change in the relative flame propagation speed; 2) the most important result of the interaction process is the change in the flame-front structure; and 3) the amplification of the propagation velocity of the flame is associated with the breakup of its front into a space distributed reaction zone.

Nomenclature

a = sound velocity
A = a_y/a_x
A_x = a_x/a_0
c_p = specific heat
M = local Mach number
M_0 = V/a_0
p = pressure
P = p_y/p_x
q = heat of reaction per unit mass
Q = q/a_0^2
t = time
T = temperature
u = particle velocity
ΔU = $(u_y - u_x)/a_0$
U = u_y/a_0
V = relative wave velocity
w = $u + V$, absolute wave velocity
x = distance
γ = ratio of specific heats

Subscripts

0 = reference state of undisturbed region
1, x = states ahead of wave
2, y = states behind wave

Introduction

DURING recent years the study of shock-flame interaction processes has attracted a good deal of attention. The field of inquiry, however, remained somewhat confused. The reason for this was perhaps the fact that there has been inadequate communication between the theoretical and the experimental investigators. As a consequence the experimental observations that contributed toward an understanding of some details of the interaction process were culminated by only qualitative interpretation of results. Moreover, although most experiments were based on the use of photographic techniques and pressure transducer records, the correlation between the two sets of measurements has never been really exploited. Finally, only a limited amount of success was reported on the quantitative gasdynamic interpretation of experimental observations.

The purpose of the present paper is to coordinate the available information on the subject and to delineate specifically its salient features. It contains, consequently, a critical review of the literature and a set of photographic and pressure transducer records obtained in our laboratory, together with their complete quantitative analysis.

Since we are concerned essentially with shocks that have been generated by accelerating flames, the paper represents a logical sequel to our previous publications dealing with the problems of the generation of pressure waves by the flame[1] and of the ensuing formation of the shock wave.[2] In the present investigation, attention has been directed specifically at the effects of the interactions rather than the course of their progress. In other words, this study applies to the case in which the duration and extent of the interaction processes are small in comparison with the field of observation, so that enough time and space are provided for the transient phenomena to die down before each subsequent interaction event takes place.

The object is, then, to evaluate stationary states that are created by the interactions between shocks and flames in a detonative gas under the constraint of a constant cross-sectional area of the detonation tube. Under these conditions the attainment of stationary states is manifested by the appearance of straight-line wave-front traces (world-lines) in the time-distance plane of a streak schlieren record. Several examples are presented to demonstrate that, subject to this restriction, the consequences of the interactions can be explained quite satisfactorily in terms of the gasdynamic effects, provided that proper allowance is made for a finite change in the normal propagation speed of the flame.

Review of Previous Work

One of the early theoretical investigations of flame-shock interactions was accomplished by Chu,[3] who demonstrated that, if the flame propagation speed is assumed to remain constant, the shock wave becomes attenuated as the result of the interaction with the flame.

The first experiments designed specifically to study a single flame-shock interaction were reported by Markstein,[4, 5] who used a shock tube with provisions for independent control of both the shock wave and the laminar flame undergoing a head-on collision process. On the basis of schlieren ob-

Received August 10, 1964; revision received December 7, 1964. This research was supported by the United States Air Force, through the Air Force Office of Scientific Research of the Air Research and Development Command under Grant No., AFOSR-129-64 and through NASA under Grant No. NsG-10-59.

* Associate Research Engineer. Member AIAA.
† Assistant Research Engineer. Member AIAA.
‡ Professor of Aeronautical Sciences. Fellow Member AIAA.

servations he concluded that the interaction process proceeds in two stages. First, transmitted and reflected waves are established without significant alteration in the flame-front structure. Then, after a short time lag, the flame surface distorts in response to the shock-induced acceleration, producing an increase in the rate of heat release that is associated with the generation of secondary pressure waves. Although the first stage is amenable to gasdynamic analysis, the second presents a more complicated problem, partially caused by its transient nature and especially by the lack of information concerning the response of the flame surface to impulsive accelerations. The modified Taylor instability criterion proposed by Markstein[6] to explain his experimental observations represents one of the few significant contributions to this problem.

The experiments of Markstein inspired Rudinger to formulate the algebraic principles for the shock-flame interaction analysis.[7] This marked the only instance of a promising coordination between experiment and analysis. Unfortunately the investigators did not have the opportunity to bring their studies to a point permitting the attainment of quantitative conclusions.

The method of Rudinger requires an iterative process and is consequently quite time consuming. The treatment is considerably simplified by the assumption that the pressure drop across the flame is negligible. Although this corresponds to the technically important case of moderate flame speeds, it definitely limits the scope of the analysis.

In view of the complicated nature of flame response, Rudinger restricted his attention to the first phase of the interaction. In contrast to Chu[3] he took into account the temperature dependence of the flame speed by assuming that, to the first approximation, it is proportional to the absolute temperature of the medium into which the flame propagates. Under the idealizations of constant heat of reaction per unit mass and constant specific heats, this leads to the condition of constant particle velocity change across the flame. Under such circumstances it turns out that the flame behaves essentially as a contact discontinuity between the hot and cold gases.

The lack of information on flame response to flow disturbances was strongly emphasized by Rudinger. Because of their technical importance to propulsion systems, he indicated in particular the need for studies involving turbulent flames.§

In recent years, interactions between flames and shock waves became a subject of extensive study in the USSR. In the course of an investigation of high-frequency combustion instability, Shchelkin[8, 9] developed a criterion for shock-wave amplification based on a model of a weak, plane shock interacting with a highly idealized model of a square wave flame front. The experimental observations of Salamandra,[10] based on the use of both streak and repetitive flash schlieren techniques, revealed much information on the interaction process including, in particular, the response of the flame surface to the induced accelerations. In essence these results resembled those of Markstein,[5] and, similarly as in his case, the mechanism of the breakup of the flame owing to the action of the incident shock wave, and its influence on the propagation speed of the combustion wave, remained unresolved problems.

As a result of their studies the Soviet investigators became convinced that the interaction process should be treated as one comprised of three, rather than only two, distinct phases: 1) the flame acting first as a pure interface, separating hot and cold gases, for which the shock interaction effects can be computed without any difficulty; 2) the amplification of transmitted and reflected shock waves as a result of the increase in the rate of heat release during the interaction between the shock and the reaction zone; and 3) further generation of pressure waves that occurs when the flame surface distorts in response to the accelerating effects of the shock wave.

The second phase of the interaction has been studied especially by Kogarko et al.,[11–13] who derived an expression for an amplification coefficient defined in terms of the ratio of the reaction time to that of the interaction process. They concluded[11] that amplification occurs only when this quantity becomes sufficiently small.

Novikov and Riazantsev[14] carried out a gasdynamic analysis reminiscent of the approach of Chu[3] and Rudinger.[4] They applied a perturbation technique to the fundamental conservation equations of the flame front, considering the flame speed as a function of only the pressure and temperature of the unburned mixture. This led to an expression for the acoustical impedance of the flame front. In addition to the impedance of the pure interface, it was comprised of terms accounting for the effects of 1) chemical reaction, 2) entropy discontinuity between the reflected wave and the flame, and 3) change in the flame speed. The first and third terms included a coefficient whose sign and magnitude determined the extent of the amplification. Even for the case of constant flame speed the effect of the flame front was manifested by the entropy disturbance created behind the reflected shock wave.

In a recent publication Salamandra and Sevastyanova[15] reported on an experimental study of flame-shock interactions performed with the use of an ingeneously simple technique for the production of the incident shock wave. A constant area tube, filled with hydrogen-oxygen mixtures at various initial pressures, was provided with two spark ignitors, one located at the center of the test section and the other at one end of the duct. The mixture was ignited first at the end of the tube, where the accelerating flame generated a shock whose arrival in the test section was synchronized with the discharge of the second spark. The second ignition source produced two flames moving in opposite directions, and the incident shock was then doubly refracted during the interaction, colliding first with the incoming flame and, after traversing the burned gases, overtaking the receding flame. Observations were made by means of streak schlieren photography. The amplification of the shock was expressed as the ratio of the Mach numbers of the wave in the unburned medium after and before the interaction. Since the photographic reproduction of the shock wave propagating through the reaction products is as a rule poor, and the composition and temperature of the products cannot be determined accurately, this method circumvented most of the problems associated with the study of single interactions.

Results of calculations were cited, without reporting their details, however, in order to demonstrate that the observed phenomena could not be explained if the flame were treated as an interface. Although the relaxational mechanism of Kogarko and Skobelkin[11] was described as a possible explanation of the shock-wave amplification, no attempt was made to apply this theory quantitatively.

In the absence of any evidence in this respect, we have analyzed the results of Salamandra and Sevastyanova, using the vector polar method, to demonstrate that the observed amplification is consistent with the gasdynamic effects of the interaction, provided that proper allowance is made for the change in the flame propagation speed.

Vector Polar Method

A considerable simplification in the computing procedure for the evaluation of shock-flame interactions can be obtained by the use of the vector polar method[17]—a graphical technique for the solution of finite wave interaction problems which has been particularly useful in analyzing the events that occur in the course of the development of detonation.[18, 19]

§ It is of interest to note that, in his recent review on gaseous detonations, Soloukhin[16] reiterated the same opinion, pointing out in particular the importance of gathering more information about the deformation of the flame that is induced by the interaction process.

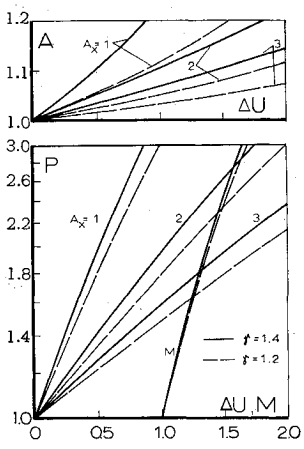

Fig. 1 Shock polars for $\gamma = 1.4$ and $\gamma = 1.2$.

The method admits only changes in state brought about by the wave action. Since it neglects wave structure, it can be described best as a method concerned only with effects "in the large" rather than with details "in the small" of the interaction process. However it can take into account the variation of all parameters without any simplifying assumptions.

In the case of the flame-shock interaction, proper consideration can be given to the pressure drop as well as to the change in particle velocity and their functional dependence on the speed of propagation of the reaction front; moreover no restrictions need be placed on the strength of the shock wave. Although an iterative procedure is still required, the primary advantage of the method is the relative rapidity with which the graphical technique leads to the solution. Its major drawback, on the other hand, is the loss of generality such as that afforded by the analytical approaches of Chu and Rudinger or Novikov and Riazantsev.

The vector polar method utilizes polar curves in the pressure-velocity and local velocity of sound-particle velocity hodograph planes. The use of the logarithm of pressure ratio as the ordinate instead of the conventional linear scale imparts a vectorial character to the hodograph plane. The polar curve then is the locus of end points of vectors having state (0, 0) as common origin, whose one component is the nondimensional particle velocity change $\Delta U = (u_x - u_y)/a_0$, and whose other component is the logarithm of pressure ratio $P \equiv p_x/p_y$ across the wave, subscripts x and y denoting the states ahead of and behind the wave, respectively. Thus each subsequent state is determined as a sum of vectors representing the changes resulting from the action of wave fronts that form the initial boundaries of its regime in the time-space plane. For a given substance, and under the restrictions of a particular process, each polar is a function only of the local velocity of sound of the medium into which the wave propagates.

The algebraic background of the method has been described in our earlier publications.[17, 18] Introduced here are the polar diagrams drawn to scale for the particular thermodynamic properties pertaining to the operating conditions of our experiments.

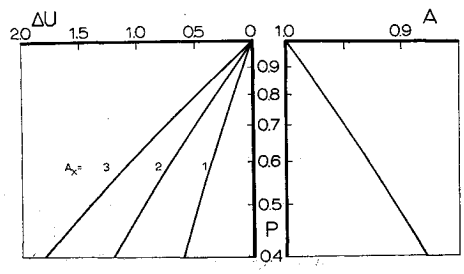

Fig. 2 Rarefaction polars for $\gamma = 1.4$.

Shock Polars

The lower diagram of Fig. 1 represents shock polars in the P-U plane for $\gamma = 1.4$ and $\gamma = 1.2$, the latter shown by broken lines. Each curve corresponds to a given value of the nondimensional velocity of sound $A_x \equiv a_x/a_0$ of the medium into which the shock propagates, subscript 0 denoting the state of the undisturbed medium taken as the reference condition. In addition the polars include curve M relating the ratio of wave velocity to the local velocity of sound, i.e., relating the local Mach number of the wave front to the pressure ratio.

The upper diagram of Fig. 1 represents shock polars in the plane of the sound velocity ratio and the nondimensional particle velocity. The ordinate $A \equiv a_y/a_x$ is plotted to a linear scale, so that this plane does not have a vectorial character of hodograph. All curves are plotted to scale and refer to a shock wave moving to the right.

Rarefaction Polars

Figure 2 represents the rarefaction polar in the P-U plane for the case of a perfect gas with $\gamma = 1.40$ and also refers to the wave moving to the right. As in the case of the shock polars, each curve of the family corresponds to a constant value of the nondimensional local velocity of sound of the medium into which the rarefaction propagates. The rarefaction wave appears in the time-space domain as a fan whose leading edge propagates into the medium at a velocity equal to the local velocity of sound and whose trailing edge leaves behind the substance at a relative velocity corresponding also to the local velocity of sound. The additional curve on the right-hand side of Fig. 2 is an auxiliary plot of the ratio of the local sound velocities $A \equiv a_y/a_x$ as a function of the pressure ratio $P \equiv P_y/P_x$.

Deflagration Polars

The deflagration polar in the P-U plane is shown as the lower diagram in Fig. 3. It is plotted for an equimolar hydrogen-oxygen mixture considered as a perfect gas with $\gamma_1 = 1.4$, $\gamma_2 = 1.2$, and the heat of reaction $q = 931$ cal/g. The values of these parameters, established on the basis of our previous studies,[3] provide a self-consistent and sufficiently accurate description of the thermodynamic properties of the products. As in the previous cases, the deflagration polar is plotted for a wave moving to the right. On the right-hand

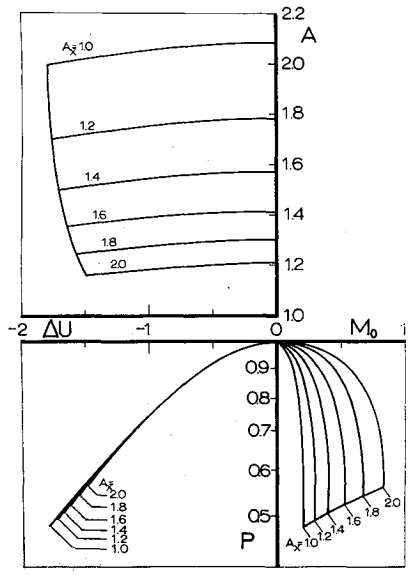

Fig. 3 Deflagration polars for $\gamma_1 = 1.4$, $\gamma_2 = 1.2$, and $Q = 19.3$.

side of Fig. 3 are the nondimensional wave velocities $M_0 \equiv V/a_0$.

The upper diagram of Fig. 3 is a linear plot of the sound speed ratio as a function of the change in particle velocity across the flame. All curves are terminated by the lower Chapman-Jouguet state, that is, when the local Mach number becomes unity.

Interaction Between a Shock and a Constant Pressure Deflagration

The application of the vector polar method can be illustrated most simply by considering the case of the interaction between a shock and a constant pressure deflagration. This serves here also as a demonstration that the condition of constant particle velocity change across the flame reduces the effects of the deflagration to those of a contact discontinuity.

The process is shown in Fig. 4. Its wave diagram in the time-space domain is on the right, and the corresponding pressure hodograph plane is on the left. The flame, denoted by the broken line, propagates to the right into the undisturbed state 0. It brings about a finite change in particle velocity creating state 1 (to the left of state 0 on the U axis) into which the incident shock propagates. The state of the medium behind it, represented by point 2, is located on the shock polar emanating from point 1.

As a result of the interaction there is obtained a reflected shock R creating state 3, a transmitted shock T creating state 4, and the disturbed flame creating state 3a. States 3 and 3a differ in the value of the local velocity of sound and entropy but not in pressure and particle velocity (hence the advantage of the P–U plane). The interface between them or contact discontinuity is denoted by C. The locus of states 3 is given by a "left" shock polar emanating from point 2; the locus of states 4 is given by a "right" shock polar emanating from point 0.

If the change in particle velocity across the flame remains unaltered, the states denoted by points 3 and 4 on the P–U diagram of Fig. 4 are attained as a result of the interaction. In the case of a contact discontinuity the shock polar emanates from point 0 rather than 1, but retains the same shape. Hence the distance between the corresponding state points 2′ and 2 is equal to ΔU and, since the reflected shock polar becomes then shifted to the right only by the same amount, the transmitted shock creates an identical state 4 as before. Thus a constant pressure deflagration with the particle velocity change unaffected by the interaction process behaves essentially as a contact discontinuity.

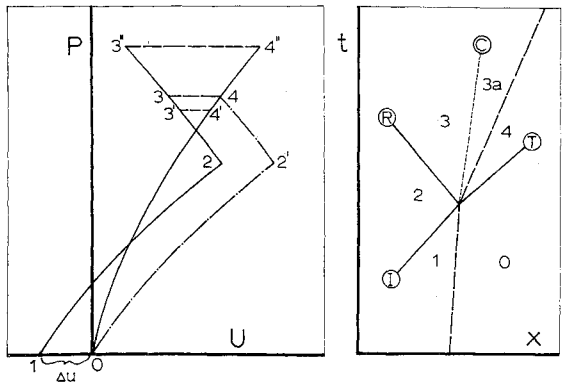

Fig. 4 Hodograph and time-space diagrams of shock wave overtaking a constant pressure deflagration. States 3 and 4 denote flame with constant velocity change which produces the same result as pure interface. States 3′ and 4′ refer to constant velocity flame, whereas states 3″ and 4″ show consequences of the increase in flame propagation speed.

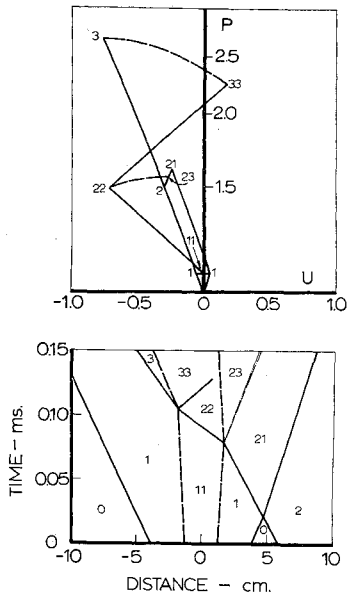

Fig. 5 Finite wave analysis of flame-shock interaction in equimolar hydrogen-oxygen mixture reported by Salamandra and Sevastyanova.[15] Dashed line denotes flame front, solid lines represent shock waves; the rarefaction wave is indicated by the chained dotted lines.

For a constant pressure deflagration it follows from the continuity equation and the energy equation that, in the case of a perfect gas with constant specific heat c_p,

$$\Delta U = \frac{M_0}{A_x^2} \frac{q}{c_p T_0}$$

where T_0 is the reference temperature. Since as a rule A_4 is higher than A_0, the assumption of constant flame speed M_0 leads to the decrease in ΔU, as shown in Fig. 4 by points 3′ and 4′. It is apparent on the diagram that the transmitted shock is then weaker than in the case of a contact discontinuity, confirming the analytical results of Chu.[3] Finally it becomes obvious that, in order to obtain an amplification of the transmitted shock with respect to that resulting from the interaction with a contact discontinuity, the change in

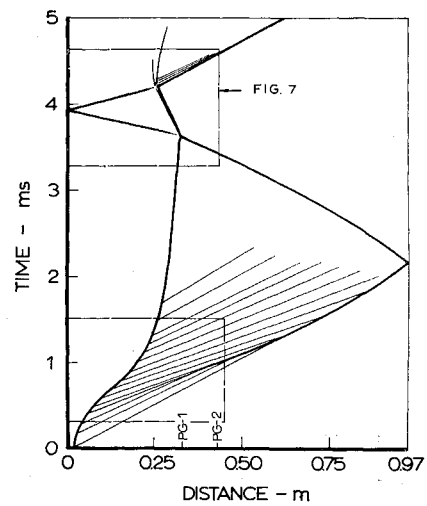

Fig. 6 Time-space diagram depicting events observed by streak schlieren photographs. Ignition by glow coil at left-hand end of tube produces an accelerating flame, represented by the heavy curved line, preceded by a collapsing pressure wave, shown as a family of thin straight lines. The shock waves that are formed reflect from the far end and undergo multiple interactions with the flame. The process of initial flame acceleration, delineated by dashed lines forming the lower rectangle, is discussed in Ref. 1; the regime of the interaction, defined by the upper rectangle, forms the subject of the current study.

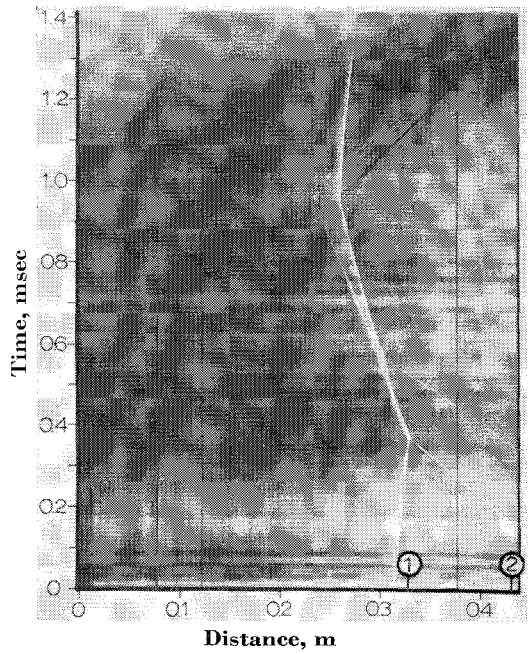

Fig. 7 Streak schlieren photograph of regime of interaction delineated in Fig. 6 by the upper dash rectangle labeled Fig. 7. Time is referenced to the instant the light was flashed on.

particle velocity across the flame must increase, as shown by points 3″ and 4″ in Fig. 4.

It should be noted, as can be verified easily by the reader, that identical results are obtained in the case of head-on collision between a shock and a deflagration.

Analysis of Experimental Observations of Salamandra and Sevastyanova[15]

Specific application of the vector polar method is demonstrated by the quantitative analysis of the experimental results reported by Salamandra and Sevastyanova, who observed the interaction process between a shock and a flame in an equimolar hydrogen-oxygen mixture.

The results of our analysis are shown on the time-space diagram and the pressure-particle velocity hodograph plane in Fig. 5. The solid lines represent shock fronts, the dashed lines refer to the flame, and the chain dotted lines delineate the rarefaction fan.

The continuous compression wave ahead of the flame front was approximated here by a discrete shock wave whose strength was determined by the velocity of the flow behind it, reported to be four-tenths of the measured flame speed. Starting with the initial flame 1–11, the shock wave preceding it 0–1, and the incident shock front 0–2, the analysis yielded the coordinates of state 3 behind the shock wave transmitted through the reaction zone. For this purpose the reported amplification factor $M_3/M_1 = 1.3$ was used, establishing at the same time the strength of the deflagration behind the transmitted shock. In this manner the analytical flame velocity was found to be 422 m/sec, which agreed quite well with the speed observed by Salamandra and Sevastyanova immediately following the interaction. Subsequent acceleration of the flame, clearly evident on the schlieren photograph, resulted from the increase in the flame-front area which was caused by the passage of the shock front. Results of the analysis are summarized in Table 1. All of them are quite consistent with experimental observations.

Experiment

The experiments were performed with equimolar hydrogen-oxygen mixtures maintained initially at room temperature and 100 mm Hg. The mixture was contained in a 1- × $1\frac{1}{2}$-in. rectangular cross-section detonation tube and ignited by means of an electrically heated glow coil.

The operating conditions were the same as those of our study of the initial generation of pressure waves by the accelerating flame,[1] and the results were sufficiently reproducible that the two sets of observations could be combined to give a complete history of the process, as shown in Fig. 6. Ignition by the glow coil produced an accelerating flame preceded by a collapsing pressure wave, forming shock waves which reflected from the far end of the tube and underwent multiple interactions with the flame. The regime of the streak schlieren observations of the nonsteady process of initial flame acceleration, discussed in the previous paper,[1] is delineated in Fig. 6 by dashed lines forming the lower rectangle; the scope of the current study is defined by the upper rectangle.

A streak schlieren photograph of the regime of interaction is shown in Fig. 7. Two shock waves moving to the left collide with the right moving flame, the first sweeping the flame back toward the left end of the tube and the second producing a noticeable alteration of its structure. Following reflection from the end of the tube, the transmitted shocks interact again with the flame, accelerating it to the right.

Pressure records obtained at two positions indicated in Fig. 7 are presented in Fig. 8. The pressures were measured by means of shock-mounted Kistler-Corporation-type 601 transducers with type 568 charge amplifiers. The first signal on both transducer records represents the pressure pulse produced by the initial motion of the flame. This is followed by the attainment of a relatively uniform pressure field ahead of the flame just prior to the interaction.

The salient feature of the schlieren record (Fig. 7) is the appearance of relatively straight line traces of wave fronts, providing the justification for the finite wave interaction analysis in which the flow is treated essentially as one-dimensional and the only changes of state admitted are those brought about by wave action. The waves are considered as plain discontinuities with the exception of the rarefaction

Table 1 State and wave parameters of Fig. 5

State	P	A	U	Wave	M	V	$U + V$	w, m/sec
0	1	1	0	...	...	...	...	...
1	1.067	1.03	0.052	0–1	1.03	1.03	1.03	463
11	1.067	2.56	0	1–11	...	0.0775	0.1295	58.2
2	1.51	1.06	−0.3	0–2	−1.2	−1.2	−1.2	− 540
21	1.61	1.092	−0.25	1–21	−1.2	−1.24	−1.19	− 535
23	1.55	1.08	−0.27	21–23	1.0	1.092	0.84	378
					1.0	1.08	0.81	364
22	1.495	2.60	−0.72	23–22	...	0.1	−0.17	− 76.5
		2.7		11–22	−1.18	−3.02	−3.02	−1360
3	2.67	1.7	−0.77	0–3	−1.56	−1.56	−1.56	− 700
33	2.24	2.2	0.18	3–33	...	−0.17	−0.94	− 422
		2.71		22–23	1.21	3.15	2.43	1095

fan, which is treated as a zone of continuous isentropic expansion. Thus all considerations associated with the structure of the wave processes are neglected in favor of their dynamic effects.

Analysis

The solution of the wave-interaction analysis is shown in the time-space diagram of Fig. 9 and the pressure-particle velocity hodograph of Fig. 10. The flame is denoted in Fig. 9 by the double solid line and the shock fronts by single solid lines; the edges of the rarefaction fan are indicated by chain-dotted lines. For comparison, the observations of Fig. 7 have been reproduced in Fig. 9, the flame trace represented by a double-dash line and the shock waves by a single-dashed line.

Each regime in the time-space domain is denoted by a number which indicates its thermodynamic state in the pressure-velocity hodograph. In performing the analysis, the contact surfaces generated by each interaction were ignored since their effects were of second order and had negligible influence on the results.

The initial conditions for the analysis are first established on the basis of experimental data as follows. As shown in Fig. 6, immediately after ignition the flame accelerated for approximately 1.0 msec, then decelerated, probably as a result of its contact with the walls of the tube, acquiring eventually a constant velocity of 48 m/sec (Fig. 7). The motion of the flame produced a pressure pulse appearing on the left-hand side of both pressure records in Fig. 8. This led to the establishment of state 1—a regime of a relatively uniform state ahead of the constant velocity flame front. The pressure of state 1 was taken as 2.01 psi, the mean of the values measured at positions 2 and 3 (Fig. 8) and, because it was created by a simple wave, its particle velocity of 13 m/sec was deduced from the Riemann invariance.

The first incident shock wave on the schlieren photograph (Fig. 7) appeared to be followed immediately by a weaker, barely discernible shock. However, since the second front could not be resolved on the pressure transducer record, its effects were ignored, and the incident wave was represented by a single front whose pressure and velocity provided the best fit with the experimental record.

State 1 and the waves 1–2, 2–4, and 1–11 provided the initial conditions for the analysis. For convenience the reference conditions were taken as those of the undisturbed mixture, so that state 1 was slightly displaced from the origin of the P-U diagram (Fig. 10).

Curve 1–2 represents the locus of states attained behind the shock wave propagating to the left into medium 1, with the terminal point state 2 determined from the observed pressure and wave velocity. Curve 1–11 represents the locus of states

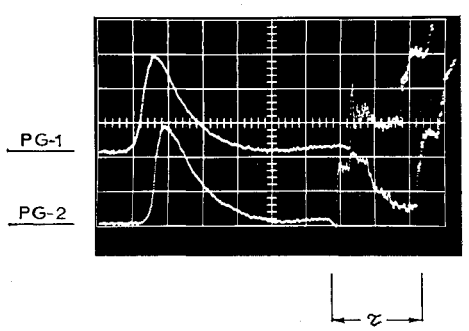

Fig. 8 Pressure records obtained at positions indicated in Fig. 7. Vertical scale: 1 cm = 0.5 psi; horizontal scale 1 cm = 500 μsec from left to right. Signal on left-hand side of figure represents pressure pulse produced by initial motion of flame. τ indicates the time interval of 1.4 msec during which the schlieren record (Fig. 7) was obtained.

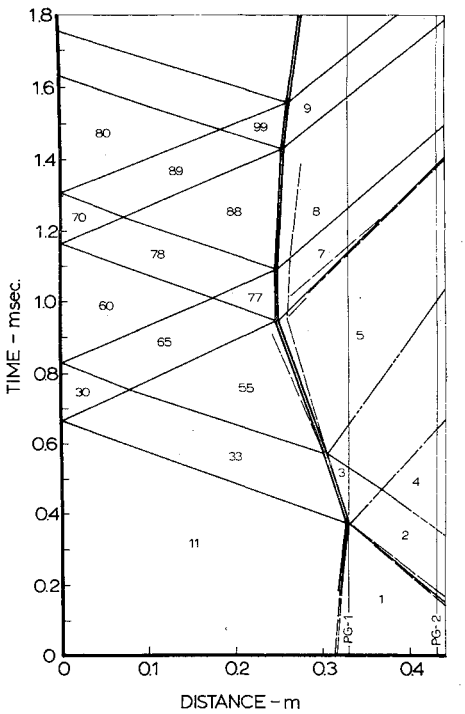

Fig. 9 Time-space diagram of flame-shock interactions showing results of the finite wave analysis. The observed flame is represented by the thin double-dashed lines. The analytical flame is shown as the double solid lines. The positions of the pressure transducers are denoted by the vertical lines labeled PG-1 and PG-2.

created behind the deflagration moving to the right into medium 1. State 11 is specified by the deflagration polar of Fig. 4 to fit the observed flame velocity.

The rarefaction produced by the collision between the first incident shock wave 1–2 and flame 1–11 was considered to be "spread out" along the path of the flame until it collided with the second incident shock 2–4. This was consistent with the continuous generation of pressure waves by flame 3–33, as observed on the schlieren photograph and with the expansion process indicated on the pressure records which, as shown later, could not be explained in terms of a rarefaction centered at the point of collision. The continuous generation of the rarefaction wave was most probably caused by the flattening of the flame front by the shock-induced accelerations.

The rarefaction that arose from the collision between flame 3–33 and shock 2–4 was a weak wave. It was considered in this case to be centered at the point of collision, and its effects were combined with those of the first expansion. As a consequence there appeared an extended regime of uniform state 5, in agreement with experimental observations. Although flame 3–33 propagated into the nonuniform regime within the reflected rarefaction wave, the medium ahead of it was assumed to have a constant state 3 whose properties cor-

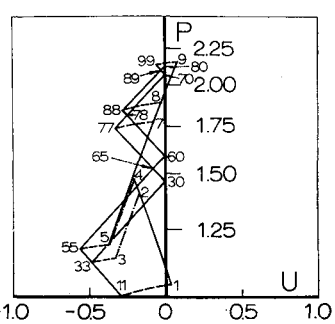

Fig. 10 Nondimensional pressure-particle velocity hodograph. The numbered state points correspond to the stationary flow regimes indicated in Fig. 9.

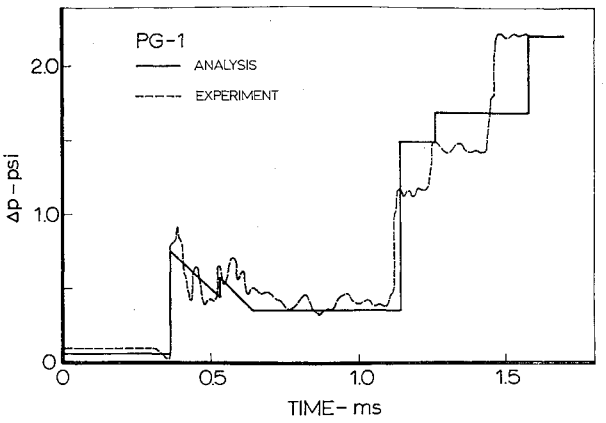

Fig. 11 Comparison of experimental and analytical pressure profiles at position PG-1 indicated in Fig. 9.

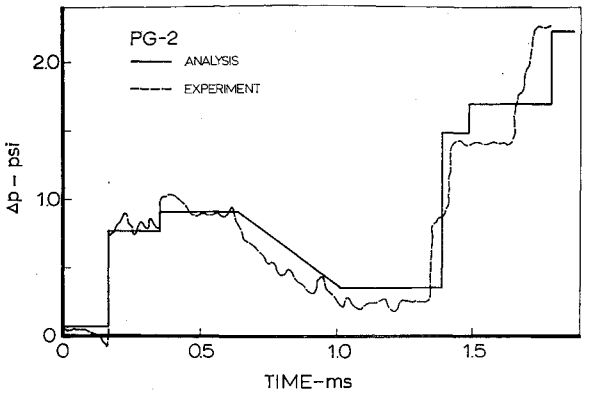

Fig. 12 Comparison of experimental and analytical pressure profiles at position PG-2 indicated in Fig. 9.

responded to those behind the rarefaction produced by the first flame-shock collision. This should be considered a fair approximation, especially in view of experimental evidence. The rarefaction waves attributed to changes in flame shape propagated in both directions so that shock 11–33 was actually followed by an expansion that tended to "smear out" the subsequent interactions. For purposes of analysis, however, and in keeping with the assumptions stated earlier, state 33 was considered uniform with properties corresponding to those behind the transmitted shock wave after it was overtaken by the weaker rarefaction.

States 3 and 33 were determined on the P-U plane of Fig. 10 by closing the pentagon whose remaining vertices were located at state points 11, 1, and 2. A unique solution was obtained by requiring that the velocity of the transmitted deflagration 3–33 match the flame world-line on the schlieren record, whereas point 33 was the same as that behind the transmitted shock 11–33. The results of such a solution are quite approximate since the pressure and velocity changes across the deflagration are sensitive to small deviation in flame velocity. However, an upper bound to state 3, and hence state 33, is provided by state 5 (which, together with state 55, is found in a similar fashion as are states 3 and 33), whose pressure was recorded by both pressure transducers.

A further check on the solution for states 5, 33, and 55 arose from the fact that they served as starting points for the remainder of the analysis which was particularly sensitive to the location of these state points in the P-U plane. Hence, when the calculated pressures of states 7, 8, and 9, and velocities of waves 5–7, 7–8, 8–9, 7–77, and 8–88, did not agree with experimental observations, slight changes were made in states 3, 5, 33, and 55 until the best over-all match between analysis and experiment was obtained.

The key to the success of the analysis, it should be emphasized, was the allowance for the flame speed to change as a consequence of each interaction.

Table 2 State and wave parameters of Figs. 9 and 10

State	P	ΔP, psi	A	U	Wave	M	V	$U+V$	w, m/sec
1	1.04	0.075	1.0056	+0.028	0–1	...	0	0.028	13
2	1.393	0.76	1.05	−0.17	1–2	−1.14	−1.145	−1.117	− 502
11	1.003	0.005	2.085	−0.29	1–11	...	0.078	0.106	48
3	1.133	0.26	1.02	−0.33	2–3	1	1.05	0.88	392
						1	1.02	0.69	310
33	1.119	0.23	2.19	−0.485	11–33	−1.05	−2.19	−2.48	−1120
					3–33	...	0.035	−0.295	− 133
4	1.47	0.91	1.06	−0.21	2–4	−1.024	−1.075	−1.25	− 563
5	1.185	0.36	1.03	−0.375	4–5	1	1.06	0.85	
						1	1.03	0.655	+ 294
55	1.168	0.325	2.19	−0.56	5–55	...	0.040	−0.335	− 150
					33–55	−1.02	−2.235	−2.720	−1225
30	1.447	0.865	2.24	0	33–30	1.13	2.53	2.045	920
65	1.514	0.995	2.25	−0.08	30–65	−1.02	−2.29	−2.29	−1030
					55–65	1.135	2.55	1.99	896
60	1.576	1.115	2.25	0	65–60	1.02	2.29	2.21	995
7	1.77	1.495	1.09	−0.07	5–7	1.190	1.30	0.925	915
77	1.725	1.405	2.27	−0.33	7–77	...	0.07	0	0
					65–77	−1.065	−2.42	2.50	−1125
8	1.88	1.70	1.10	−0.025	7–8	1.03	1.12	1.05	472
88	1.84	1.62	2.28	−0.28	8–88	...	0.07	0.0450	22
					78–88	−1.01	−2.30	−2.555	1150
78	1.803	1.55	2.28	−0.255	77–78	1.02	2.32	1.99	896
					60–78	−1.06	−2.46	−2.46	1100
70	2.065	2.06	2.30	0	78–70	1.06	2.42	2.165	972
89	2.095	2.12	2.30	−0.03	88–89	1.06	2.42	2.14	962
					70–89	1.008	−2.32	−2.32	−1045
80	2.125	2.17	2.31	0	89–80	1.008	2.32	2.29	1030
9	2.15	2.22	1.12	0.08	8–9	1.06	1.165	1.14	512
99	2.125	2.17	2.32	−0.06	9–99	...	0.03	0.11	50
					89–99	−1.007	−2.32	−2.35	−1060

Conclusions

The results of the analysis are summarized in Table 2. The time-space diagram (Fig. 9) was used then to evaluate pressure variations at the locations of the two pressure transducers. The resulting profiles are shown in Figs. 11 and 12, where the experimental pressure records have been also reproduced.

General features of the analytical and experimental pressure profiles, such as timing and relative amplitude, are in satisfactory agreement. The discrepancy between the two curves, which becomes especially evident at later stages of the interaction, can be attributed to a number of factors. Besides the idealizations concerning the thermodynamic properties of the medium, the effects of the reflected rarefactions as well as contact discontinuities have been neglected in the analysis; the continuous wave processes, such as the generation of pressure waves by the flame when it was distorted in response to the shock-induced accelerations, have not been taken into account; and the influence of the wire coil that formed the ignitor on the shock waves reflected from the end of the tube has been disregarded.

In view of the good agreement obtained here, it can be concluded that the effects of multiple shock-flame interactions can be explained quite satisfactorily by means of gasdynamic analysis, provided that proper allowance is made for a finite change in the relative flame propagation speed. Amplification of the resulting wave-train, in comparison to that which arises when the flame is considered as a pure interface, is obtained, in fact, as a direct consequence of the increased rate of heat release which is associated with the increase in the propagation velocity.

The most important effect of the interaction process is, therefore, the resulting change in the flame-front structure produced by the shock-induced accelerations, since amplification of the propagation velocity is associated, as a rule, with the breakup of the flame front into a distributed reaction zone.

Finally, it should be noted that the finite wave interaction analysis is conservative in that it produces slightly higher pressures than those actually measured.

References

[1] Urtiew, P. A., Laderman, A. J., and Oppenheim, A. K., "Dynamics of pressure wave generation by an accelerating flame," *Proceedings of the Tenth Symposium (International) on Combustion* (Combustion Institute, Pittsburgh, Pa., in press).

[2] Laderman, A. J., Urtiew, P. A., and Oppenheim, A. K., "On the generation of a shock wave by flame in an explosive gas," *Ninth Symposium (International) on Combustion* (Academic Press Inc., New York, 1963), pp. 265–274.

[3] Chu, B. T., "On the generation of pressure waves at a plane flame front," *Fourth Symposium (International) on Combustion* (Williams and Wilkins Co., Baltimore, Md., 1953), pp. 603–612.

[4] Markstein, G. H. and Schwartz, D., "Interaction between pressure waves and flame fronts," Jet Propulsion **25,** 173–174 (1955).

[5] Markstein, G. H., "A shock-tube study of flame front-pressure wave interaction," *Sixth Symposium (International) on Combustion* (Reinhold Publishing Corp., New York, 1957), pp. 387–398.

[6] Markstein, G. H., "Flow disturbances induced near a slightly wavy contact surface, or flame front, traversed by a shock wave," J. Aeronaut. Sci. **24,** 238 (1957).

[7] Rudinger, G., "Shock wave and flame interactions," *Third AGARD Colloquium Combustion and Propulsion* (Pergamon Press, New York, 1958), pp. 153–176.

[8] Shchelkin, K. I., "O vozmozhnom mekhanisme usileniya slabykh udarnykh voln v zone turbulentnogo goreniya" ("On the possible mechanism of amplification of weak shock waves in the zone of turbulent combustion"), Izv. Akad. Nauk SSSR, Otd. Teckhn. Nauk Energ. i Avtomat. **5,** 86–96 (1959).

[9] Shchelkin, K. I. and Troshin, Ya. K., *Gasdynamics of Combustion* (Academy of Sciences, Moscow, USSR, 1963); also NASA TTF-231 (October 1964).

[10] Salamandra, G. D., "Interaction between a flame and a shock discontinuity," ARS J. **30,** 73–76 (1960); transl. from Physical Gasdynamics, USSR Acad. Sci.

[11] Kogarko, S. M. and Skobelkin, V. I., "Relaksatsionnoye vzaimodeistviye udarnykh voln s zonoi goreniya" ("Relaxational interaction of shock waves with the combustion zone"), Dokl. Akad. Nauk SSSR **120,** 1280–1283 (1958).

[12] Kogarko, S. M., Skobelkin, V. I., and Kazakov, A. N., "Vzaimodeistviye udarnykh voln s frontom plameni" ("Interaction of shock waves with the flame front"), Dokl. Akad. Nauk SSSR **122,** 1046–1348 (1958).

[13] Kogarko, S. M., "Amplification of compression waves in the combustion zone," *Eighth Symposium (International) on Combustion* (Williams and Wilkins Co., Baltimore, Md., 1962), pp. 1159–1164.

[14] Novikov, S. S. and Riazantsev, Yu. S., "Vzaimodeistviya slabykh voln davleniya s frontom plameni" ("Interaction of weak pressure waves with the flame front"), Dokl. Akad. Nauk SSSR **137,** 6, 1409–1412 (1961).

[15] Salamandra, G. D. and Sevastyanova, I. K., "Formation of weak shock waves ahead of a flame front and their intensification during passage through the flame," Combust. Flame **7,** 169–174 (1963).

[16] Soloukhin, R. I., "Detonation waves in gases," Usp. Fiz. Nauk. **80,** 525–551 (1963); transl. in Soviet Phys.—Usp. **6,** 523–541 (1964).

[17] Oppenheim, A. K., Urtiew, P. A., and Laderman, A. J., "Vector polar method for the evaluation of wave interaction processes," Arch. Machine Design, Polish Academy of Sciences **II,** 441–495 (1964).

[18] Oppenheim, A. K. and Stern, R. A., "On the development of gaseous detonation—analysis of wave phenomena," *Seventh Symposium (International) on Combustion* (Butterworths Scientific Publications, London, 1959), pp. 837–850.

[19] Laderman, A. J. and Oppenheim, A. K., "Influence of wave reflections on the development of detonation," Phys. Fluids **4,** 778–782 (1961).